AMERICAN JOURNAL OF PHYSICAL ANTHROPOLOGY 140:234–243 (2009)

Discrimination of Extant *Pan* Species and Subspecies Using the Enamel–Dentine Junction Morphology of Lower Molars

Matthew M. Skinner,[1,2]* Philipp Gunz,[1] Bernard A. Wood,[2] Christophe Boesch,[3] and Jean-Jacques Hublin[1]

[1]*Department of Human Evolution, Max Planck Institute for Evolutionary Anthropology, Leipzig 04103, Germany*
[2]*Center for the Advanced Study of Hominid Paleobiology, Department of Anthropology, George Washington University, Washington, DC, 20052*
[3]*Department of Primatology, Max Planck Institute for Evolutionary Anthropology, Leipzig 04103, Germany*

KEY WORDS tooth morphology; micro-computed tomography; geometric morphometrics; sliding semilandmarks

ABSTRACT Previous research has demonstrated that species and subspecies of extant chimpanzees and bonobos can be distinguished on the basis of the shape of their molar crowns. Thus, there is potential for fossil taxa, particularly fossil hominins, to be distinguished at similar taxonomic levels using molar crown morphology. Unfortunately, due to occlusal attrition, the original crown morphology is often absent in fossil teeth, and this has limited the amount of shape information used to discriminate hominin molars. The enamel–dentine junction (EDJ) of molar teeth preserves considerable shape information, particularly in regard to the original shape of the crown, and remains present through the early stages of attrition. In this study, we investigate whether the shape of the EDJ of lower first and second molars can distinguish species and subspecies of extant *Pan*. Micro-computed tomography was employed to non-destructively image the EDJ, and geometric morphometric analytical methods were used to compare EDJ shape among samples of *Pan paniscus* ($N = 17$), *Pan troglodytes troglodytes* ($N = 13$), and *Pan troglodytes verus* ($N = 18$). Discriminant analysis indicates that EDJ morphology distinguishes among extant *Pan* species and subspecies with a high degree of reliability. The morphological differences in EDJ shape among the taxa are subtle and relate to the relative height and position of the dentine horns, the height of the dentine crown, and the shape of the crown base, but their existence supports the inclusion of EDJ shape (particularly those aspects of shape in the vertical dimension) in the systematic analysis of fossil hominin lower molars. Am J Phys Anthropol 140:234–243, 2009.

Molar crown morphology has been used to address taxonomic questions in extant apes (Johanson, 1974; Hartman, 1988; Uchida, 1992, 1996, 1998a,b; Pilbrow, 2003, 2006) and fossil hominins (e.g., Robinson, 1956; Sperber, 1974; Wood and Abbott, 1983; Wood et al., 1983, Wood, 1991; Suwa et al., 1994, 1996; Suwa, 1996; Grine, 2004, Bailey, 2006, Martinón-Torres et al., 2006, 2008; Skinner et al., 2008a). The taxonomic distinctiveness of molar crown shape has most recently been demonstrated by Pilbrow (2003, 2006), who, based on a large number of linear crown measurements, was able to distinguish between species, subspecies, and even populations of African apes (particularly chimpanzees).

Quantitative analyses of the shape of fossil hominin teeth are frequently limited to gross linear dimensions (e.g., buccolingual and mesiodistal diameter of the crown), cusp surface areas, and crown base shape. While these can yield a reasonable degree of discrimination between certain taxa, considerable overlap often remains, limiting the taxonomic level at which closely related taxa can be distinguished. Among the variably worn teeth of fossil samples, many aspects of tooth crown shape that might distinguish taxa cannot be measured due to an inability to defend them as being homologous between specimens.

It has long been acknowledged that the enamel–dentine junction (EDJ), which underlies the enamel cap of primate teeth, carries information about the original shape of the tooth crown (Kraus, 1952; Korenhof, 1960, 1961, 1982; Nager, 1960; Kraus and Jordan, 1965; Sakai et al., 1965, 1967a,b, 1969; Sakai and Hanamura, 1971, 1973a,b; Corruccini, 1987a,b, 1998; Schwartz et al., 1998; Sasaki and Kanazawa, 1999; Skinner, 2008; Skinner et al., 2008b) and that it can be used as a source of taxonomically relevant data (Corruccini, 1998; Olejniczak et al., 2004, 2007; Macchiarelli et al., 2006; Suwa et al., 2007; Skinner et al., 2008a, 2009). Furthermore, it is homologous among teeth and taxa and is preserved throughout the initial stages of tooth wear (and longer in the thicker-enameled and low-cusped molars of many archaic hominin taxa). The goal of this project was to assess the taxonomic distinctiveness of the EDJ morphology of lower molars in extant species and subspecies

Grant sponsors: NSF IGERT; EVAN Marie Curie Research Training Network MRTN-CT-019564; Max Planck Society.

*Correspondence to: Matthew M. Skinner, Department of Human Evolution, Max Planck Institute for Evolutionary Anthropology, Deutscher Platz 6, Leipzig 04103, Germany.
E-mail: skinner@eva.mpg.de

Received 22 October 2008; accepted 28 January 2009

DOI 10.1002/ajpa.21057
Published online 20 April 2009 in Wiley InterScience (www.interscience.wiley.com).

of *Pan*. If it can be demonstrated that the *Pan* EDJ can distinguish these taxonomic levels, then it is likely that the same method can be used to discriminate species of the other genera within the *Pan*/*Homo* clade (Skinner et al., 2008).

Two species of chimpanzee are commonly recognized: *Pan paniscus* and *Pan troglodytes*. *P. paniscus*, also referred to as the bonobo or pygmy chimpanzee, is found in the Democratic Republic of the Congo and all but the southern limits of its range are defined by the Congo River. The species distinction between *P. paniscus* and *P. troglodytes* has been supported by both morphological (e.g., Coolidge, 1933; Johanson, 1974; Shea et al., 1993; Uchida, 1996, Pilbrow, 2006) and molecular studies (Morin et al., 1994; Ruvolo et al., 1994; Won and Hey, 2005; Becquet et al., 2007). There are a number of commonly recognized subspecies of *P. troglodytes* whose ranges are separated by geographic barriers from other *Pan* populations: *Pan troglodytes verus* (western chimpanzees—separated by the Dahomey gap), *Pan troglodytes vellorosus* (Nigerian chimpanzees—separated by the Sanaga River), *Pan troglodytes troglodytes* (central chimpanzees—separated by the Ubangi River), and *Pan troglodytes schweinfurthii* (eastern chimpanzees—separated by the Ubangi River and Congo River). While the subspecies distinction of each of these taxa is debated (Fischer et al., 2006) and is more strongly supported for some taxa (e.g., *P. t. verus*) than for others (e.g., the distinction between *P. t. troglodytes* and *P. t. schweinfurthii*), both morphological (Johanson, 1974; Shea et al., 1993; Uchida, 1996, Pilbrow, 2003, 2006) and molecular evidence (Morin et al., 1994; Stone et al., 2002; Won and Hey, 2005; Gonder et al., 2006; Becquet et al., 2007) supports their distinction. Furthermore, both morphological and genetic evidence suggest that *P. t. verus* is the most distinctive (either due to earlier genetic isolation or smaller effective population size) of the subspecies.

Based on the results of previous studies that have demonstrated the distinctiveness of external molar crown shape among species and subspecies of *Pan* and the evidence that the EDJ contributes significantly to crown shape (Korenhof, 1960; Kraus and Jordan, 1965; Corruccini, 1987a, 1998; Skinner, 2008), we test the hypothesis that the EDJ morphology of lower first and second molar crowns can successfully distinguish extant *Pan* species and subspecies. Support for this hypothesis would suggest that the factors that have led to a divergence in tooth shape between taxa act when the shape of the EDJ is being established early in tooth development. Lack of support for this hypothesis would suggest that EDJ morphology carries a more conservative taxonomic signal and that differences in enamel growth are responsible for the findings of previous studies of the distinctiveness in shape of the external molar crown.

In order to test this hypothesis, we perform a geometric morphometric analysis of anatomical landmarks collected on the surface of the EDJ. The EDJ surface of each molar is non-destructively imaged using micro-computed tomography (microCT). Anatomical landmarks are chosen to capture the overall crown shape of the EDJ, including crown height, dentine horn height (dentine horns are the conical structures that underlie cusps on the outer enamel surface), dentine horn spacing, and the shape of the cervix. Not only does this methodology allow the quantitative assessment of shape differences among taxa, but it also provides visual depictions of the shape differences that may distinguish taxa. We assess the accuracy with which molars are correctly classified to their known taxonomic affiliation and examine metameric variation in EDJ shape between M_1 and M_2.

MATERIALS AND METHODS

Study sample

The sample includes *P. paniscus* (Pp; $M_1 = 8$ and $M_2 = 9$) and two subspecies of *P. troglodytes* (Pt), *P. t. troglodytes* (Ptt; $M_1 = 7$ and $M_2 = 6$) and *P. t. verus* (Ptv; $M_1 = 8$ and $M_2 = 10$). The Ptt sample derives from the Museum für Naturkunde (ZMB) in Berlin, Germany and the subspecies designation is inferred from the localities (located in Cameroon or Gabon) from which the specimens originate. The Ptv sample comes from a skeletal collection housed at the Max Planck Institute for Evolutionary Anthropology in Leipzig, Germany comprising deceased individuals collected within the research mandate of the Taï Chimpanzee Project based in the Taï National Park, Republic of Côte d'Ivoire. The subspecies designation is based on the fact that only Ptv is present in this area. The Pp sample derives from the Royal Museum for Central Africa (MRAC) in Tervuren, Belgium. Species designation is based on locality information and museum catalogue information associated with each specimen. Thirteen additional molars (3 from MRAC and 10 from ZMB), whose taxonomic affiliation below the genus level is unknown, were also included in the study, and they were classified using information from the taxonomically identified samples.

Micro-computed tomography

Each tooth was microCT scanned using a SKYSCAN 1172 Desktop Scanner (100 kV, 94 mA, 2.0 mm aluminum and copper filter, 0.12 rotation step, 360 degrees of rotation, 2 frame averaging). Raw projections were converted into TIFF image stacks using NRecon (parameters: ring artifact correction = 10; beam hardening = 30%). Pixel dimensions and slice spacing of the resultant images ranged between 10 and 20 micrometers (μm). To reduce the size of the resulting files, teeth were resampled to a resolution of 30 μm using Amira 4.1 (www.amiravis.com; Triangle filter).

EDJ surface reconstruction

To facilitate tissue segmentation, the complete image stack for each molar was filtered using a three-dimensional median filter (kernel size of 3) followed by a mean of least variance filter (kernel size of 3), implemented as a computer-programmed macro. This results in more homogenous tissue classes (e.g., enamel vs. dentine) and replaces the intermediate gray-scale values of pixels at tissue interfaces (i.e., air–enamel, enamel–dentine, and air–dentine) with those closer to the mean value of air, enamel, or dentine based on neighboring pixels (Schulze and Pearce, 1994). Filtered image stacks were imported into Amira and enamel and dentine tissues were segmented using the 3D voxel value histogram and its distribution of gray-scale values. After this filtering step there is a marked shift in gray-scale values across the EDJ which minimized subjectivity in determining its location.

After segmentation, the EDJ was reconstructed as a triangle-based surface model using Amira (surface generation module using unconstrained smoothing parame-

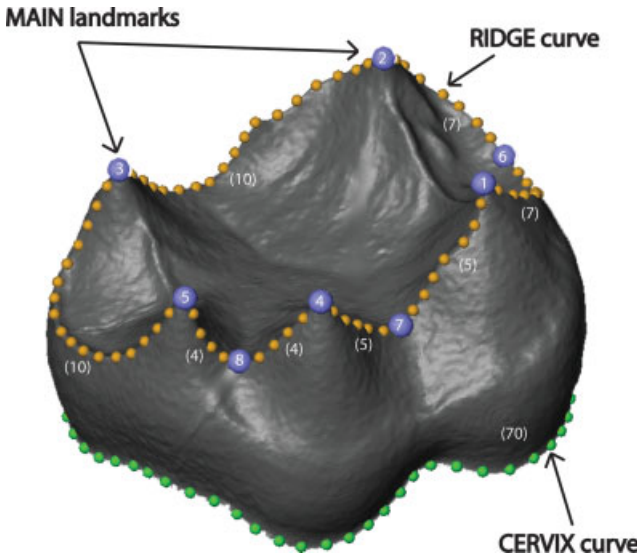

Fig. 1. EDJ surface model of a lower molar illustrating the anatomical landmarks used to capture EDJ shape. MAIN landmarks are collected on the tips of the dentine horns and in the troughs between the mesial and buccal dentine horns (large spheres). An arbitrary number of points were collected along the RIDGE curve that runs between the dentine horns and around the CERVIX curve (small spheres). Numbers in brackets refer to the interpolated semilandmarks equally spaced within each section of the RIDGE curve and along the CERVIX curve (see text for details). Points illustrated here are representative of those collected on the original specimens and are not the same as the interpolated semilandmarks. A color version of this figure can be found in the online version of this paper.

ter). Small portions of the EDJ were missing in some molars, and in these cases the defects were corrected digitally using the software Geomagic Studio v.10 (www.geomagic.com). Molars that showed evidence of significant damage or missing areas were excluded from the study. In a few minimally worn molars the tips of the dentine horns were repaired (fill holes module in Geomagic Studio).

Collection of landmarks

The EDJ surface models were imported into Amira for the collection of three sets of 3D anatomical landmarks (see Fig. 1). The first set (referred to as "MAIN") included eight landmarks: one on the tip of the dentine horn of each primary cusp [i.e., protoconid (1), metaconid (2), entoconid (3), hypoconid (4) and hypoconulid (5)], one at the mid-point on the marginal crest connecting the protoconid and metaconid (6), and one on the lowest point on the marginal ridges between the protoconid and hypoconid (7), and the hypoconid and hypoconulid (8), respectively. Landmarks were not collected in the trough between the metaconid and entoconid, or between the entoconid and hypoconulid because of the variable presence of accessory cusps in these areas.

The second set (referred to as the "RIDGE" curve) includes coordinates (~50–70) along the tops of the ridges that connect the five dentine horns. This set of points forms a continuous line, beginning at the tip of the protoconid and moving in a lingual direction. In the case of teeth with accessory cusps (e.g., cusp 6 or cusp 7) points were collected on either side of these dentine horns. The third set (referred to as the "CERVIX" curve) includes coordinates (~40–50) along the cervix, or cementum-enamel junction, of the tooth crown. This set of points also forms a closed ellipse, beginning below the protoconid dentine horn and moving in a lingual direction. Where small fragments of enamel were missing, the cervix location was estimated. As a cubic spline function is fitted to these sets of coordinates (see below), it is not initially necessary that the same number of points be placed along a curve for each specimen. Thus, the spacing of points was dictated such that they did not touch adjacent neighbors, but where not so far apart as to misrepresent aspects of the curve after spline interpolation (as represented in Fig. 1).

Derivation of homologous landmarks

Structures considered homologous are assumed to have a common evolutionary origin (Zelditch et al., 2004), but in geometric morphometrics the term 'homologous landmark' means that the landmark corresponds to the same location on the same homologous structure in different specimens, species, or developmental stages. Unlike the eight MAIN landmarks, the rest of the coordinates that make up the RIDGE and CERVIX sets, also known as 'semilandmarks' (Bookstein, 1997), are not homologous (e.g., they differ between specimens in number and in the precise location of the nth landmark along the curve). The process by which a single homologous set of landmarks was generated for each specimen was as follows. First, for both the RIDGE and CERVIX curve coordinate sets a smooth curve was interpolated using a cubic spline function (a cubic spline is used so that the curve is forced to pass through each measured coordinate). A cubic spline was fitted by starting at an initial point (being the tip of the protoconid dentine horn for the RIDGE curve and below the base of the protoconid dentine horn for the CERVIX curve) and moving lingually around the curve.

In the case of the RIDGE curve, the eight MAIN homologous landmarks were projected onto the curve dividing the curve into eight sections. For each section, a large sample of very closely spaced coordinates was computed along the curve, and the distances between adjacent coordinates were calculated and summed together to approximate the length along the curve between the MAIN landmarks. Each length was divided by a given number, based on an estimate of the relative contribution of each section to the RIDGE curve across the molars in the study sample, and the coordinate location at each equally spaced distance was recorded (the number of semilandmarks between MAIN landmarks are illustrated in brackets in Fig. 1). In the case of the CERVIX curve, its length was calculated in the same way and 70 equally spaced coordinates were derived. Thus, at this stage, all specimens have the same total number of landmarks (i.e., the homologous, fixed, landmarks on the tips of the dentine horns, plus equal numbers of semilandmarks.

We used the algorithm described by Gunz et al. (2005) that allows semilandmarks to slide along tangents to the curve. These tangents were approximated for each semilandmark as the vector between the two neighboring points. Semilandmarks were iteratively allowed to slide along their respective curves (i.e., RIDGE curve [n = 52] and CERVIX curve [n = 70]) to minimize the *bending energy* of the thin-plate spline interpolation function

computed between each specimen and the Procrustes average for the sample. After the application of the sliding algorithm, each set made up of 8 fixed landmarks and 122 semilandmarks is treated as being homologous for the purpose of multivariate analyses.

Each homologous set of landmarks was converted to shape coordinates by generalized least squares Procrustes superimposition (Gower, 1975; Rohlf and Slice, 1990). This removed information about location and orientation from the raw coordinates and standardized each specimen to unit centroid size, a size-measure computed as the square root of the sum of squared Euclidean distances from each (semi)landmark to the specimen's centroid (Dryden and Mardia, 1998). All data preprocessing was done in Mathematica v6.0 (www.wolfram.com) using a software routine written by PG.

Analysis of EDJ shape

A permutation test was used to test for statistical significance of mean shape differences between molars of each taxon (M_1 and M_2 of each of *P. paniscus*, *P. t. troglodytes* and *P. t. verus*). In each permutation ($n = 5000$) the group label of each molar was randomly reassigned and the Procrustes distances between the means of the scrambled groups was calculated. Actual group means were considered statistically significantly different if less than 5% of the permutations of random group assignments yielded Procrustes distances that were as large as those between actual group means. Principal component analysis (PCA) of shape coordinates (Bookstein, 1991; Rohlf, 1993) was used to examine overall shape variation in the sample and the distribution of each group in shape space. Canonical variate analysis (CVA), which generates linear combinations of variables that maximize the ratio of between-group to within-group variation, was used to assess the accuracy with which molars were correctly classified to taxon. The CVA computation requires the number of variables to be smaller than the number of specimens (n), and ideally the number of variables should be much smaller than n. We therefore used principal component analysis to reduce the dimensions of our dataset and computed the CVA from a subset of PCA scores (8–12) of the classified specimens. The choice to use a subset of PCs is a compromise between including a sufficient proportion of overall shape variation (~80% for each analysis) and not using too many variables so as to risk unrealistic and unstable levels of discrimination. We evaluated the impact of the choice of eight PCs by performing a CVA of randomized data created by randomly re-labeling each specimen. Using 8–12 PCs did not result in the type of spurious clustering that can occur when the ratio of sample size to the number of variables is low (see example in Skinner, 2008). To assess the accuracy with which molars were classified to taxon and molar position, we used a cross-validation approach in which each specimen was considered unknown and then classified based on the remaining sample. Increasing or decreasing the number of PCs used for the computation of the CVA can lead to different classifications for the same specimen. Therefore we report the classification accuracy for each analysis using each of 8–12 PCs. The PCA, CVA, and classifications were implemented in R and groups were assigned equal prior probabilities.

Thirteen molars, whose specific and subspecific affiliation is uncertain, were classified using the canonical variate scores generated from the 48 molars of known taxonomic affiliation in the primary study sample. Again, classification of unknown specimens can change as the number of PCs used to generate the canonical variate axes is increased or decreased. To be conservative we interpreted the classification results for the unknown specimens as follows. If the classification to taxonomic group was consistent, based on CVAs using each of 8–12 PCs, then that classification was accepted. If classification to taxonomic group was ambiguous using each of 8–12 PCs then the specimen is considered unclassified for that analysis.

Visualization of EDJ shape variation

To visualize the shape variation between taxa and among the molar positions, we employed a method which allows a 3D triangulated surface reconstruction of the EDJ to be deformed to match the mean configuration of each molar position for each taxon (Gunz et al., 2005; Gunz and Harvati, 2007). First, several thousand points were measured on the EDJ of one specimen (specimen: Pp M_1 MRAC_29026) and converted to a triangulated surface using Geomagic Studio 10. Because no shape data were collected within the occlusal basin of the EDJ this area of the surface was purposely cleaned of distinctive features. We then warped the vertices of this surface into Procrustes space using the thin-plate spline interpolation function between the landmark configuration of this specimen and the Procrustes average configuration of the whole sample. Finally, we computed a thin-plate spline between this mean configuration and each target form (e.g., the mean configuration of the Ptv M_1 sample) to produce a surface model of the appropriate mean shape. In order to visualize the taxonomic differences at each molar position the mean shapes were superimposed in Amira with one surface rendered transparent for better visual comparison.

RESULTS

Using a permutation test of the group labels, all groups are significantly different ($P < 0.05$) from each other in full shape space and in the subspace of the first ten principal components. The PCA and CVA of Procrustes shape coordinates of the first molar sample are illustrated in Figure 2. The combination of overlap in the PCA and marked separation along the first two CV axes indicates that there are consistent, but small scale, differences in shape between the taxa. Using a cross-validation analysis of the CV scores the accuracy of classification to species and subspecies is 100% and 87–100%, respectively (Table 1). These results support our hypothesis regarding the taxonomic distinctiveness of EDJ shape for first molars.

The mean shape of Pp M_1s compared to the mean shape of the combined Pt M_1 sample is visualized in Figure 3a. This represents the shape differences at the species level and includes a relatively narrower trigonid and wider talonid (particularly in the more distal placement of the entoconid and hypoconulid) in Pt compared to Pp and a reduction in the relative height of the talonid dentine horns in Pt compared to Pp. The mean shape differences in the two subspecies, Ptt and Ptv, are illustrated in Figure 3c. Ptt M_1s exhibit a relatively taller dentine crown, taller dentine horns, and a nar-

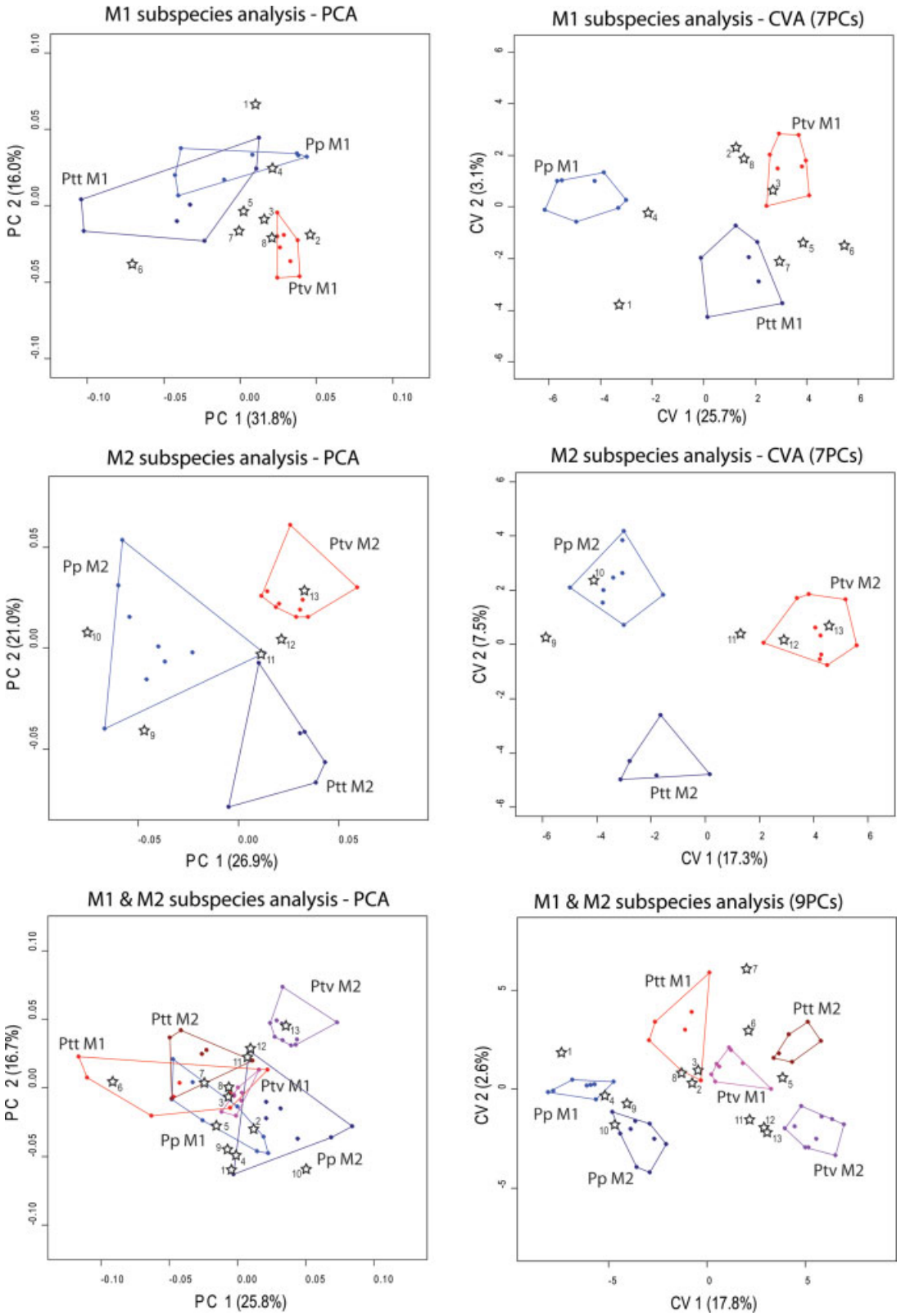

Fig. 2. Plots of the principal component analyses (PCA) and canonical variates analyses (CVA) performed on the first molar, second molar and combined molar samples of the three study taxa (Pp, *Pan paniscus*; Ptt, *Pan troglodytes troglodytes*; Ptv, *Pan troglodytes verus*). The number of PCs used for each CVA is reported and the percentage of total shape variation is listed in brackets for each PC or CV axis, respectively. Numbered open stars indicate the position of specimens of unknown taxonomic affiliation (see Table 2); however, spatial associations should be interpreted with caution as only two dimensions of a multidimensional shape space are represented. [Color figure can be viewed in the online issue, which is available at www.interscience.wiley.com.]

TABLE 1. Classification accuracy[a] to species and subspecies of molars with pre-established taxonomic affiliation

Analysis	Taxonomic level	Correctly classified by taxon (%)
First molars only	Species	100
First molars only	Subspecies	87–100
Second molars	Species	100
Second molars	Subspecies	100
All molars	Species	98–100
All molars	Subspecies	96–98

[a] Classification based on cross-validation of canonical variates using 8–12 principal components.

rower talonid whereas Ptv M_1s exhibit a shorter dentine crown, shorter dentine horns, and a wider talonid.

The PCA and CVA of the second molar sample are illustrated in Figure 2. As with the analysis of first molars, the first two CV axes separate the three taxa. Classification accuracy based on the cross-validation analysis of the CV scores is 100% at both the species and subspecies level (Table 1). Combining the first and second molar samples also resulted in highly accurate classification rates (92–100% at the species level and 94–98% at the subspecies level). These results support our hypothesis regarding the taxonomic distinctiveness of EDJ shape for second molars.

The mean shape of Pp M_2s compared to the mean shape of the combined Pt M_2 sample is visualized in Figure 3b. The shape differences at the species level include relatively centrally placed dentine horns in Pt M_2s compared to more laterally placed dentine horns in Pp M_2s resulting in a relatively larger occlusal basin in the latter. The hypoconulid dentine horn of Pt M_2s is also relatively smaller compared to that of Pp M_2s. The mean shape differences in M_2s of the two subspecies, Ptt and Ptv, are illustrated in Figure 3d. Ptt second molars exhibit a buccolingually narrower crown base, relatively taller dentine horns and a taller dentine crown, while Ptv molars exhibit a wider, more rectangular, crown base, a wider occlusal basin, shorter dentine horns, and a shorter dentine crown.

Patterns of metameric variation

Permutation tests of Procrustes distances between groups reveal significant mean shape differences between the first and second molar in each taxon. EDJ shape variation along the molar row in each species is illustrated in Figure 4. There are a number of consistent differences between first and second molars in each species including a reduction in relative dentine horn height, more laterally placed mesial dentine horns, and a trend towards a reduction in EDJ crown height in second molars (rendered as the solid surface).

Classification of unknown molars

In Table 2 we present the classification of 13 molars whose taxonomic affiliation is unknown beyond the level of genus. A number of these molars yield consistent taxonomic classifications in each analysis (highlighted with shading) when compared to molars of the same position or the combined molar sample. The species designation of the majority of molars was consistent with expectations based on limited provenience information and first and second molars belonging to the same individual (MRAC 84036M11 and ZMB 72844) were consistently classified the same way in each analysis. In the absence of genetic analyses of these specimens the accuracy of these classifications cannot be evaluated, but these results suggests that EDJ morphology can be examined to inform the taxonomic affiliation of unknown specimens.

DISCUSSION

The results of this study demonstrate that the EDJ shape of molars carries information useful for discriminating extant *Pan* species and subspecies. Three previous examinations of the taxonomic differences in tooth morphology of *Pan* are particularly relevant to the results of this study. The first was by Johanson (1974) who examined metric and non-metric dental variation in Pp and in the three subspecies of Pt. He noted significant differences in both metric (MD and BL dimensions) and non-metric variables between Pp and Pt and significant differences in non-metric variables among the three subspecies of Pt (but not in linear dimensions). He also noted the distinctiveness of Ptv compared to the other subspecies of Pt. Uchida (1992, 1996) examined craniodental variation among hominoids. She used linear dimensions, cusp areas, and the frequency of non-metric traits as the variables for her analyses. Her findings echoed Johanson's regarding metrical differences in lower molar morphology between Pp and Pt, but differed in that significant metrical differences were found between Ptv and Ptt. These included the relative size of the M_1 and M_2 protoconid (Ptv larger), the relative size of the M_1 and M_2 hypoconid (Ptt larger), and M_2 crown shape (Ptv relatively wider buccolingually). Cusp area measurements also distinguished Ptv from the other Pt subspecies. The distinctiveness in EDJ morphology at the species and subspecies level revealed in our analysis is consistent with these results.

Pilbrow (2003, 2006) examined morphometric variation in African ape teeth, including chimpanzee molars, using a comprehensive set of linear measurements and angles on the tooth crown. She demonstrated significant morphometric variation between species, subspecies and individual populations of *Pan*. Mahalanobis distances between populations of chimpanzee resulted in four groups consistent with Pp, Ptv, Ptt, and Pts. Based on shape variables, the classification accuracies in Pilbrow's analysis were as follows: Pp—M_1, ~70% and M_2, ~88%; Pt—M_1, ~90% and M_2, ~93%; Ptt—M_1, ~52% and M_2, ~62%; Ptv—M_1, ~80% and M_2, ~70%. Thus, the classification accuracy using our EDJ shape data is similar to, if not slightly better than, that of a study based on the OES. We suggest that this is because the methodology employed in this study captures shape variation in the vertical dimension including crown height and dentine horn height.

Taxonomic decisions that partition the hominin fossil record into hypodigms are essential for exploration of the evolutionary history and paleobiology of the hominin clade. The results we have presented indicate that EDJ morphology is distinctive at both the species and subspecies level in extant *Pan*. Thus, it is reasonable to predict that the EDJ morphology of the teeth of fossil hominins, who share a most recent common ancestor with extant chimpanzees, is also likely to preserve taxonomically relevant shape information at the same taxonomic levels.

Indeed, EDJ morphology, based on high-resolution CT images, is beginning to be used for the diagnosis of new hominid taxa (Suwa et al., 2007), and an analysis of EDJ shape in two southern African hominin taxa, *Australopithecus africanus* and *Paranthropus robustus*, indicates that lower molar EDJ morphology distinguishes both taxon and tooth type (Skinner et al., 2008a). Our results also support the continued use of OES morphology for taxonomic discrimination and emphasize the importance of capturing shape variation in the vertical dimension when possible.

Previous authors have suggested that the EDJ carries a more conservative taxonomic signal than the OES (e.g., Korenhof, 1960; Sakai and Hanamura, 1973a,b; Corruccini, 1987b; Sasaki and Hanazawa, 1999). While our results indicate that the EDJ carries a strong taxonomic signal it is difficult to assess how this relates to the taxonomic signal of the OES. This is for two reasons. First, unworn teeth are scarce, even in large museum collections, and second our methodology is difficult to apply to the OES, as the placement of landmarks on the more rounded surface of the OES is more subjective than along the sharp ridge that runs between the dentine horns. Future research into the taxonomic and phylogenetic utility of tooth structure (including EDJ and enamel cap morphology) should increase sample sizes of high-resolution EDJ data to assess expected levels of intraspecific variation. Furthermore, it may be that a combination of EDJ morphology and the morphology of the enamel cap will be most effective for distinguishing closely related taxa, as selection for external crown morphology can occur during the formation of the EDJ and/

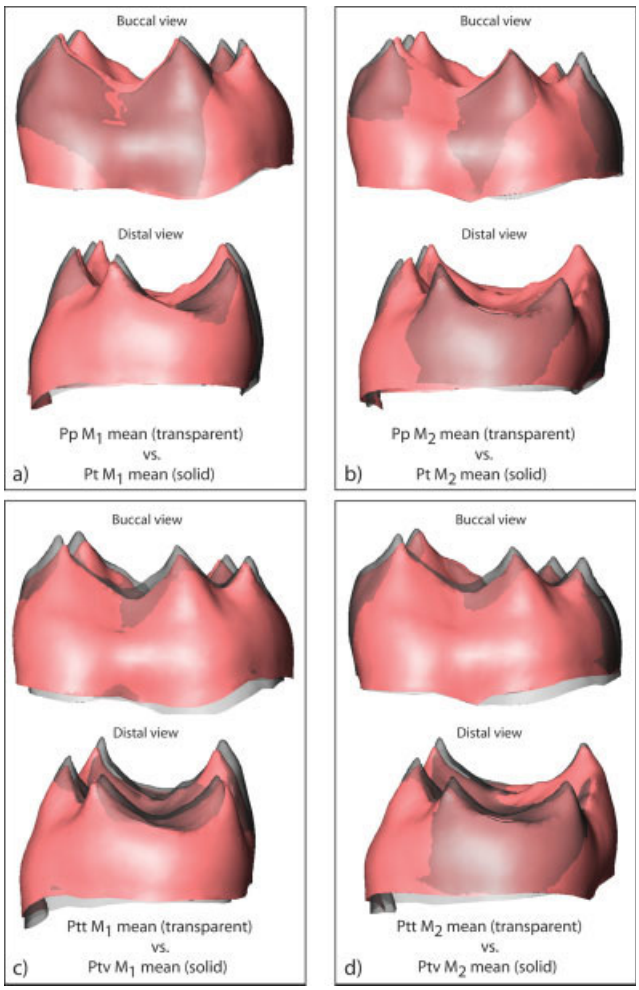

Fig. 3. Taxonomic differences in mean lower molar EDJ shape. (**a**) Species level comparison between the mean *P. paniscus* M_1 shape (transparent) and the mean shape of the combined *P. troglodytes* M_1 sample (solid). (**b**) Species level comparison between the mean *P. paniscus* M_2 shape (transparent) and the mean shape of the combined *P. troglodytes* M_2 sample (solid). (**c**) Subspecies level comparison between the mean *P. t. troglodytes* M_1 shape (transparent) and the mean *P. t. verus* M_1 shape (solid). (**d**) Subspecies level comparison between the mean *P. t. troglodytes* M_2 shape (transparent) and the mean *P. t. verus* M_2 shape (solid). Note the differences in dentine horn height and position on the EDJ.

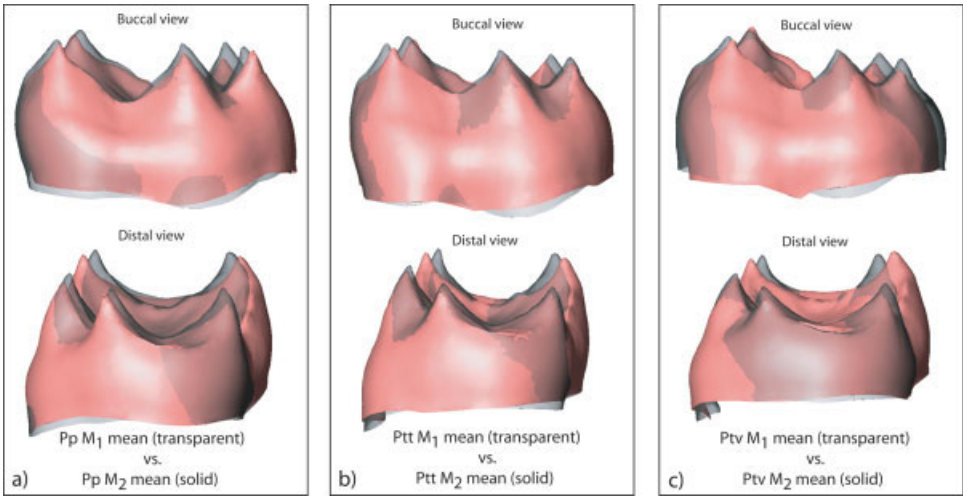

Fig. 4. Metameric variation in mean EDJ shape within each species. (**a**) *P. paniscus*; (**b**) *P. t. troglodytes*; (**c**) *P. t. verus*. For each species the mean M_1 shape (transparent) is overlain upon the mean M_2 shape (solid). Note the consistent reduction in relative dentine horn height and the more centrally located mesial dentine horns in M_2 compared to M_1.

TABLE 2. List of specimens with unknown taxonomic affiliation[a] in each analysis

#[b]	First molars	Provenience information[c]	M1 species	M1 and M2 species	M1 subspecies	M1 and M2 subspecies
1	MRAC 84036M11	Collected by the same individual as other Pp specimens	Pp	Pp	Pp	Pp
2	ZMB 0A809	None	Pt	Pt	Ptv	Ptv
3	ZMB 20811	None	Pt	Pt	Ptv	Ptv
4	ZMB 32052	"Taken on board in Matadi"	Pp	Pp	Pp	Pp
5	ZMB 32356	Katsema, Cameroon	Pt	PtM?	?	?
6	ZMB 47506	Zoo specimen from Berlin, Germany	Pt	Pt	Ptv	?
7	ZMB 6983	Listed in museum catalogue as coming from west Africa	Pt	Pt	Ptt	Ptt
8	ZMB 72844	Zoo specimen from Berlin, Germany	Pt	Pt	Ptv	Ptv
	Second molars	Provenience information	M2 species	M1 and M2 species	M2 subspecies	M1 and M2 subspecies
9	MRAC 84036M10	Collected by the same individual as other Pp specimens	Pp	Pp	Pp	Pp
10	MRAC 84036M11	Collected by the same individual as other Pp specimens	Pp	Pp	Pp	Pp
11	ZMB 24838	Bugoie forest, Rwanda	Pt	Pt	?	Ptv
12	ZMB 33489	Egypt	Pt	Pt	Ptv	Ptv
13	ZMB 72844	Zoo specimen from Berlin, Germany	Pt	Pt	Ptv	Ptv

[a] For each specimen the classification that resulted from using 8–12 PCs was assessed. That classification is listed when the classification was consistent for increasing numbers of PCs. When classification using increasing numbers of PCs differed, that specimen was considered to be of ambiguous taxonomic affiliation (?). Shaded specimens returned consistent classifications for analyses of individual molars and when the first and second molar samples were combined.
[b] Numbers at left indicate the location of specimens in the PCA and CVA plots of Figure 2.
[c] Provenience information gathered from museum records.

or be related to the distribution of enamel deposited over the EDJ.

Uchida (1996) noted that it is difficult to point out any obvious functional significance of the shape differences between extant *Pan* species and subspecies. The consistent patterns of metameric variation in EDJ shape along the molar row, including variations in the relative size and height of the dentine horns and the placement of the dentine horns across the crown, could contribute to differences in function morphology between first and second molars. Such differences may influence occlusal basin size, or the size and shape of crest features on the molar crown. However, the EDJ surface does not independently interact with food being masticated. The surface of the unworn tooth is the combination of EDJ shape and differential enamel distribution, and in partially worn teeth the worn enamel cap and areas of exposed dentine can together create functional crests (King et al., 2005). Enamel cap morphology and the correlation between the EDJ and OES will need to be assessed in each taxon to determine the extent to which EDJ shape is translated to the OES, and thus determine whether the shape of the former can be used for interpreting the function of the latter.

CONCLUSIONS

This study tested the hypothesis that the EDJ morphology of molar tooth crowns could distinguish between extant *Pan* species and subspecies. The hypothesis is supported based on the accuracy with which individual teeth are classified to the appropriate species and subspecies. Morphological differences between extant *Pan* taxa are subtle (relating primarily to the relative height and positioning of the dentine horns, but also relative crown height and crown shape) but they can be visualized by the geometric morphometric methodology employed in this study. Our results suggest that EDJ morphology carries taxonomically relevant information that can be incorporated into similar analyses of fossil hominids. Furthermore, it is clear that distinguishing hominid taxa using post-canine tooth crown morphology, and assigning isolated molars to existing or new taxa, will be facilitated by capturing as much shape information (particularly in the vertical dimension) as possible at both the enamel surface and EDJ.

ACKNOWLEDGMENTS

We thank the following museums and curators for access to specimens: Robert Asher, Hendrik Turni, and Irene Mann of the Museum für Naturkunde, Berlin, Germany; Emmanuel Gilissen and Wim Wendelen of the Royal Museum for Central Africa, Tervuren, Belgium. Heiko Temming of the MPI-EVA assisted in the microCT scanning. Gert Wollny wrote the computer macro to filter the CT images. C.B. thanks the Ministry of Environment and Eaux et Forêts, the Ministry of Scientific Research, the Direction of the Taï National Park as well as the Swiss Centre of Scientific Research for constant support to the Taï chimpanzee project. The participation of M.M.S. was supported by a George Washington University Academic Excellence fellowship. The participation of B.A.W. was supported by a GW University professorship and by the GW VPAA, Don Lehman.

LITERATURE CITED

Bailey SE. 2006. Beyond shovel-shaped incisors: Neandertal dental morphology in a comparative context. Periodicum Biologorum 108:253–267.

Becquet C, Patterson N, Stone AC, Przeworski M, Reich D. 2007. Genetic structure of chimpanzee populations. PLOS Genet 3:e66. doi:10.1371/journal.pgen.0030066.
Bookstein FL. 1997. Landmark methods for forms without landmarks: morphometrics of group differences in outline shape. Med Image Anal 1:225–243.
Coolidge HJ. 1933. *Pan paniscus*. Pygmy chimpanzee from south of the Congo River. Am J Phys Anthropol 18:1–57.
Corruccini RS. 1987a. The dentinoenamel junction in primates. Int J Primatol 8:99–114.
Corruccini RS. 1987b. Relative growth from the dentino–enamel junction in primate maxillary molars. J Hum Evol 2:263–269.
Corruccini RS. 1998. The dentino–enamel junction in primate mandibular molars. In: Lukacs JR, editor. Human dental development, morphology, and pathology: a tribute to Albert A Dahlberg. Portland: University of Oregon Anthropological Papers 54, University of Oregon. p 1–16.
Dryden I, Mardia KV. 1998. Statistical shape analysis. New York: John Wiley.
Fischer A, Pollack J, Thalmann O, Nickel B, Pääbo S. 2006. Demographic history and genetic differentiation in apes. Curr Biol 16:1133–1138.
Gonder MK, Disotell TR, Oates JF. 2006. New genetic evidence on the evolution of chimpanzee populations and implications for taxonomy. Int J Prim 27:1103–1127.
Grine FE. 2004. Description and preliminary analysis of new hominid craniodental remains from the Swartkrans Formation. In: Brain CK, editor. Swartkrans: a cave's chronicle of early man. Pretoria: Transvaal Museum. p 75–116.
Gunz P, Harvati K. 2007. The Neanderthal "chignon": variation, integration, and homology. J Hum Evol 52:262–274.
Gunz P, Mitteroecker P, Bookstein FL. 2005. Semilandmarks in three dimensions. In: Slice DE, editor. Modern morphometrics in physical anthropology. New York: Kluwer Academic, Plenum. p 73–98.
Hartman SE. 1988. A cladistic analysis of hominoid molars. J Hum Evol 17:489–502.
Johanson DC. 1974. An odontological study of the chimpanzee with some implications for hominoid evolution. Ph.D. dissertation, University of Chicago.
Korenhof CAW. 1960. Morphogenetical aspects of the human upper molar. Utrecht: Uitgeversmaatschappij Neerlandia.
Korenhof CAW. 1961. The enamel–dentine border: a new morphological factor in the study of the (human) molar pattern. Proc Koninkl, Nederl Acad Wetensch 64B:639–664.
Korenhof CAW. 1982. Evolutionary trends of the inner enamel anatomy of deciduous molars from Sangiran (Java, Indonesia). In: Kurtén B, editor. Teeth: form, function and evolution. New York: Columbia University Press. p 350–365.
Kraus BS. 1952. Morphologic relationships between enamel and dentin surfaces of lower first molar teeth. J Dent Res 31:248–256.
Kraus BS, Jordan R. 1965. The human dentition before birth. Philadelphia: Lea and Febiger.
Macchiarelli R, Bondioli L, Debénath A, Mazurier A, Tournepiche J-F, Birch W, Dean C. 2006. How Neanderthal molar teeth grew. Nature 444:748–751.
Martinón-Torres M, Bastir M, Bermúdez de Castro JM, Gómez A, Sarmiento S, Muela A, Arsuaga JL. 2006. Hominin lower second premolar morphology: evolutionary inferences through geometric morphometric analysis. J Hum Evol 50:523–533.
Martinón-Torres M, Bermúdez de Castro JM, Gómez-Robles A, Margvelashvili A, Prado L, Lordkipanidze D, Vekua A. 2008. Dental remains from Dmanisi (Republic of Georgia): morphological analysis and comparative study. J Hum Evol 55:249–273.
Morin PA, Moore JJ, Chakraborty R, Jin L, Goodall J, Woodruff DS. 1994. Kin selection, social structure, gene flow, and the evolution of chimpanzees. Science 265:1193–1201.
Nager G. 1960. Der vergleich zwischen dem räumlichen verhalten des dentin-kronenreliefs und dem schmelzrelief der zahnkrone. Acta Anat 42:226–250.
Olejniczak AJ, Martin LB, Ulhaas L. 2004. Quantification of dentine shape in anthropoid primates. Ann Anat 186:479–485.
Olejniczak AJ, Gilbert CC, Martin LB, Smith TM, Ulhaas L, Grine FE. 2007. Morphology of the enamel–dentine junction in sections of anthropoid primate maxillary molars. J Hum Evol 53:292–301.
Pilbrow V. 2003. Dental variation in African apes with implications for understanding patterns of variation in species of fossil apes. Ph.D. dissertation, New York University.
Pilbrow V. 2006. Population systematics of chimpanzees using molar morphometrics. J Hum Evol 51:646–662.
Robinson JT. 1963. Adaptive radiation in the australopithecines and the origin of man. In: Clark Howell F, Bourliere F, editors. African ecology and human evolution. Chicago: Aldine. p 385–416.
Rohlf FJ. 1993. Relative warp analysis and an example of its application to mosquito wings. In: Marcus LF, Bello E, Garcia-Valdecasas A, editors. Contributions to morphometrics. Madrid: Museo Nacional de Ciencias Naturales. p 131–159.
Rohlf FJ, Slice D. 1990. Extensions of the Procrustes method for the optimal superimposition of landmarks. Syst Zool 39:40–59.
Ruvolo M, Pan D, Zehr S, Goldberg T, Disotell TR, von Dornum M. 1994. Gene trees and hominoid phylogeny. Proc Nat Acad Sci USA 91:8900–8904.
Sakai T, Hanamura H. 1971. A morphology study of enamel–dentin border on the Japanese dentition. V. Maxillary molar. J Anthropol Soc Nippon 79:297–322.
Sakai T, Hanamura H. 1973a. A morphology study of enamel–dentin border on the Japanese dentition. VI. Mandibular molar. J Anthropol Soc Nippon 81:25–45.
Sakai T, Hanamura H. 1973b. A morphology study of enamel–dentin border on the Japanese dentition. VII. General conclusion. J Anthropol Soc Nippon 81:87–102.
Sakai T, Sasaki I, Hanamura H. 1965. A morphology study of enamel–dentin border on the Japanese dentition. I. Maxillary median incisor. J Anthropol Soc Nippon 73:91–109.
Sakai T, Sasaki I, Hanamura H. 1967a. A morphology study of enamel–dentin border on the Japanese dentition. II. Maxillary canine. J Anthropol Soc Nippon 75:155–172.
Sakai T, Sasaki I, Hanamura H. 1967b. A morphology study of enamel–dentin border on the Japanese dentition. III. Maxillary premolar. J Anthropol Soc Nippon 75:207–223.
Sakai T, Sasaki I, Hanamura H. 1969. A morphology study of enamel–dentin border on the Japanese dentition. IV. Mandibular premolar. J Anthropol Soc Nippon 77:71–98.
Sasaki K, Kanazawa E. 1999. Morphological traits on the dentino–ename junction of lower deciduous molar series. In: Mayhall JT, Heikkinen T, editors. Proceedings of the 11th International Symposium on Dental Morphology, Oulu, Finland, 1998. Oulu: Oulu University Press. p 167–178.
Schulze MA, Pearce JA. 1994. A morphology-based filter structure for edge-enhancing smoothing. In: Proceedings of the 1994 IEEE International Conference on Image Processing. p 530–534.
Schwartz GT, Thackeray JF, Reid C, van Reenen JF. 1998. Enamel thickness and the topography of the enamel–dentine junction in South African Plio-Pleistocene hominids with special reference to the Carabelli trait. J Hum Evol 35:523–542.
Shea BT, Leigh SR, Groves CP. 1993. Mulivariate craniometric variation in chimpanzees: implications for species identification in paleoanthropology. In: Kimbel WH, Martin LB, editors. Species, species concepts and primate evolution. New York: Plenum. p 265–296.
Skinner MM. 2008. Enamel–dentine junction morphology in extant hominoids and fossil hominins. Ph.D. dissertation, George Washington University.
Skinner MM, Gunz P, Wood BA, Hublin J-J. 2008a. Enamel–dentine junction (EDJ) morphology distinguishes the lower molar molars of *Australopithecus africanus* and *Paranthropus robustus*. J Hum Evol 55:979–988.
Skinner MM, Wood BA, Hublin J-J. 2009. Protostylid expression at the enamel–dentine junction and enamel surface of mandibular molars of *Paranthropus robustus* and *Australopithecus africanus*. J Hum Evol 56:76–85.
Skinner MM, Wood BA, Boesch C, Olejniczak AJ, Rosas A, Smith TM, Hublin J-J. 2008b. Dental trait expression at the

enamel–dentine junction of lower molars in extant and fossil hominoids. J Hum Evol 54:173–186.
Sperber G. 1974. Morphology of the cheek teeth of early South African hominids. Ph.D. dissertation, University of Witwatersrand.
Stone AC, Griffiths RC, Zegura SL, Hammer MF. 2002. High levels of Y-chromosome nucleotide diversity in the genus *Pan*. Proc Nat Acad Sci USA 99:43–48.
Suwa G. 1996. Serial allocations of isolated mandibular molars of unknown taxonomic affinities from the Shungura and Usno Formations. Ethiopia, a combined method approach. Hum Evol 11:269–282.
Suwa G, Kono RT, Katoh S, Asfaw B, Beyene Y. 2007. A new species of great ape from the late Miocene epoch in Ethiopia. Nature 448:921–924.
Suwa G, White TD, Howell FC. 1996. Mandibular postcanine dentition from the Shungura Formation. Ethiopia: crown morphology, taxonomic allocations, and Plio-Pleistocene hominid evolution. Am J Phys Anthropol 101:247–282.
Suwa G, Wood BA, White TD. 1994. Further analysis of mandibular molar crown and cusp areas in Pliocene and Early Pleistocene hominids. Am J Phys Anthropol 93:407–426.
Uchida A. 1992. Intra-species variation among the great apes: implications for taxonomy of fossil hominoids. Ph.D. dissertation, Harvard University.
Uchida A. 1996. Craniodental variation among the great apes. Cambridge, MA: Peabody Museum of Archaeology and Ethnology, Harvard University.
Uchida A. 1998a. Variation in tooth morphology of *Gorilla gorilla*. J Hum Evol 34:55–70.
Uchida A. 1998b. Variation in tooth morphology of *Pongo pygmaeus*. J Hum Evol 34:71–79.
Won Y-J, Hey J. 2005. Divergence population genetics of chimpanzees. Mol Biol Evol 22:297–307.
Wood BA, Abbott SA. 1983. Analysis of the dental morphology of Plio-Pleistocene hominids. I. Mandibular molars: crown area measurements and morphological traits. J Anat 136: 197–219.
Wood BA, Abbott SA, Graham SH. 1983. Analysis of the dental morphology of Plio-Plesitocene hominids. II. Mandibular molars—study of cusp areas, fissure patterns and cross sectional shape of the crown. J Anat 137:287–314.
Zelditch ML, Swiderski DL, Sheets HD, Fink WL. 2004. Geometric morphometrics for biologists. New York: Elsevier Academic Press.